J|A|C|S ARTICLES

Published on Web 01/13/2009

Micrometer- and Nanometer-Scale Photopatterning Using 2-Nitrophenylpropyloxycarbonyl-Protected Aminosiloxane Monolayers

Shahrul A. Alang Ahmad,[†] Lu Shin Wong,[§] Ehtsham ul-Haq,[†,‡] Jamie K. Hobbs,[†,‡] Graham J. Leggett,*[,†] and Jason Micklefield[§]

Department of Chemistry, University of Sheffield, Brook Hill, Sheffield S3 7HF, U.K., Department of Physics and Astronomy, University of Sheffield, Hicks Building, Hounsfield Road, Sheffield S3 7RH, U.K., and School of Chemistry and Manchester Interdisciplinary Biocentre, The University of Manchester, 131 Princess Street, Manchester M1 7DN, U.K.

Received September 25, 2008; E-mail: Graham.Leggett@Sheffield.ac.uk

Abstract: An approach to nanopatterning is reported in which a scanning near-field optical microscope coupled to a near-UV laser is used to selectively deprotect 2-nitrophenylpropyloxycarbonyl (NPPOC)-protected aminosiloxane monolayers on glass. UV deprotection was studied for unpatterned samples using X-ray photoelectron spectroscopy (XPS) and contact angle measurements. Highly efficient photodeprotection of the NPPOC moiety was observed upon irradiation at both 325 and 364 nm, and complete deprotection was found to occur within minutes. The resulting amine-terminated surfaces were then derivatized using trifluoroacetic anhydride (TFAA) and aldehyde-functionalized polymer nanoparticles. Contact angle and XPS measurements postderivatization indicated that surface functionalization was extensive, with the NPPOC-deprotected surfaces and aminopropylsiloxane control materials exhibiting essentially identical characteristics. Micrometer-scale patterns were fabricated using mask-based exposure, functionalized with polymer nanoparticles, and characterized by atomic force microscopy. Nanometer-scale patterns were fabricated using near-field exposure and characterized by friction force microscopy. The nanopatterns were derivatized with TFAA. The resulting images exhibited a clear contrast inversion that was due to an inversion of surface polarity in the patterned areas and confirmed that high spatial resolution (ca. 100 nm) was readily achievable.

Introduction

One of the biggest challenges in molecular nanoscience is the integration of top-down (lithographic) and bottom-up (synthetic) fabrication methodologies. Currently, there is a critical length regime, between approximately 100 nm and the dimensions of a single biomacromolecule, in which there are no established tools for the execution of specific molecular transformations. A variety of techniques exist for the patterning of molecules and biomolecules on length scales of ca. 100 nm, including dip-pen nanolithography,[1−3] nanoshaving/nanografting,[4−6] and local oxidation,[7−10] but few offer the potential to execute chemical transformations. One approach, developed by Sagiv and co-workers, has been the development of "constructive nanolithography", in which an atomic force microscope probe, biased relative to the sample, is utilized to carry out oxidative conversion of terminal alkyl groups to carboxylate and other functionalities.[7,8] Another approach, developed in the authors' laboratory, has been to utilize near-field optical techniques. Monolayers of alkanethiols may be patterned, by photochemical conversion of alkylthiolates to alkylsulfonates in the near field and their replacement with contrasting adsorbates, with a resolution that may be as good as 9 nm—approaching the dimensions of many biomacromolecules.[11−14] Recently, other methodologies have also been demonstrated to be compatible with near-field exposure, including photoconversion of benzyl chloride terminated siloxane monolayers to carboxylic acids,[15] photoconversion of oligo(ethylene glycol) groups to aldehydes,[16,17]

[†] Department of Chemistry, University of Sheffield.
[‡] Department of Physics and Astronomy, University of Sheffield.
[§] The University of Manchester.

(1) Demers, L. M.; Ginger, D. S.; Park, S.-J.; Li, Z.; Chung, S.-W.; Mirkin, C. A. *Science* **2002**, *296*, 1836.
(2) Piner, R. D.; Zhu, J.; Xu, F.; Hong, S.; Mirkin, C. A. *Science* **1999**, *283*, 661.
(3) Jung, H.; Kulkarni, R.; Collier, C. P. *J. Am. Chem. Soc.* **2003**, *125*, 12096.
(4) Xu, S.; Laibinis, P. E.; Liu, G. Y. *J. Am. Chem. Soc.* **1998**, *120*, 9356.
(5) Liu, G. Y.; Xu, S.; Qian, Y. *Acc. Chem. Res.* **2000**, *33*, 457.
(6) Xu, S.; Liu, G. Y. *Langmuir* **1997**, *13*, 127.
(7) Maoz, R.; Frydman, E.; Cohen, S. R.; Sagiv, J. *Adv. Mater.* **2000**, *12*, 424.
(8) Maoz, R.; Frydman, E.; Cohen, S. R.; Sagiv, J. *Adv. Mater.* **2000**, *12*, 725.
(9) Liu, S.; Maoz, R.; Sagiv, J. *Nano Lett.* **2004**, *4*, 845.
(10) Gu, J.; Yam, C. M.; Li, S.; Cai, C. *J. Am. Chem. Soc.* **2004**, *126*, 8098.
(11) Sun, S.; Chong, K. S. L.; Leggett, G. J. *J. Am. Chem. Soc.* **2002**, *126*, 8098.
(12) Sun, S.; Leggett, G. J. *Nano Lett.* **2004**, *4*, 1381.
(13) Ducker, R. E.; Leggett, G. J. *J. Am. Chem. Soc.* **2006**, *128*, 392.
(14) Leggett, G. J. *Chem. Soc. Rev.* **2006**, *35*, 1150.
(15) Sun, S.; Montague, M.; Critchley, K.; Chen, M.-S.; Dressick, W. J.; Evans, S. D.; Leggett, G. J. *Nano Lett.* **2006**, *6*, 29.
(16) Ducker, R. E.; Janusz, S. J.; Sun, S.; Leggett, G. J. *J. Am. Chem. Soc.* **2007**, *129*, 14842.

Scheme 1. Proposed Mechanism of NPPOC Deprotection by UV Light, after Ref 22

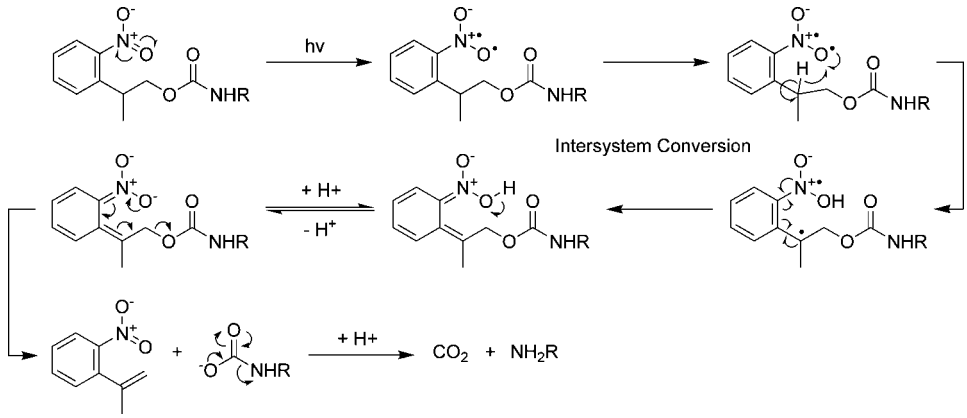

and the patterning of phosphonic acids on aluminum oxide.[18] A significant advantage offered by the use of photochemical methods is the plethora of reactions that are capable of adaptation from the extensive literature associated with photochemical synthetic methods. The present paper reports on the adaptation for nanolithography of a methodology originally developed for solid-phase synthesis of oligonucleotides.

Concomitantly, interest in the use of photolabile protecting groups to create "caged" reactive functional groups for a variety of applications, ranging from molecular electronics to biological ones, has grown steadily over the past decade.[19,20] Photocleavable protecting groups have been widely used in the synthesis of microarrays of oligonucleotides, where the exceptional efficiencies realized in photodeprotection have been critical in the execution of many repeated protection/deprotection cycles.[21−27] In this respect, nitrobenzyl-based protecting group chemistries have attracted a great deal of interest, and the *o*-nitroveratryloxycarbonyl (NVOC)[28] and α-methyl-*o*-nitropiperonyloxycarbonyl (MeNPOC)[22,29] groups are now well established in synthetic chemistry. Although suitable for the protection of carboxy and hydroxy moieties, these groups are less practical when applied to the protection of amines since carbonyl compounds are formed as photodegradation products which react with the unmasked amines to form imines.[23] Often, this must be overcome by the addition of relatively reactive carbonyl scavengers such as hydroxylamine during the deprotection step. However, the recently introduced nitrophenylpropyloxycarbonyl (NPPOC)[22] protecting group, which undergoes a different photocleavage mechanism (Scheme 1) to give an alkene byproduct, circumvents this issue and displays a superior photodeprotection efficiency.[30,31]

In the present work, the use of NPPOC-protected silane films for nanopatterning has been investigated (Scheme 2). Although there has been extensive work on patterning of alkylthiolate self-assembled monolayers (SAMs) on gold, there has been very much less work on nanofabrication on oxide surfaces. However, oxide surfaces (especially glass) offer many advantages for applications in bionanotechnology, including the absence of the fluorescence quenching effects associated with gold surfaces and their optical transparency. Monolayers of siloxanes offer the additional advantage of exceptional stability. The use of a surface protecting group strategy with established utility for biomolecular patterning at larger length scales, combined with the capacity for nanopatterning through application of near-field methods, thus presents an attractive route to the fabrication of nanostructures on oxide surfaces for a wide range of applications. Here, the synthesis of an NPPOC-protected siloxane adsorbate **1** is described (see Scheme 3), and the conditions required to prepare well-defined monolayers on silicon dioxide are investigated. The deprotection and subsequent patterning of these monolayers at length scales from the macroscopic to the nanoscale are described, and clear evidence is provided for the efficacy of near-field lithographic techniques in creating molecular nanostructures using photodeprotection methods on these surfaces.

Experimental Section

Materials. Absolute ethanol (HPLC grade, Fischer) and trifluoroacetic anhydride (>99%, Aldrich) were used as received. Triethylamine (>99%, BDH Chemicals Ltd.) was dried over molecular sieves (4 Å, Fluka) for a minimum of 72 h prior to use. Tetrahydrofuran (THF) and toluene were supplied by the Grubbs dry solvent system. Glass coverslips (Chance Proper, 22 mm × 64 mm, no. 2 thickness) and silicon (100) wafers (Goodfellow, Cambridge, U.K.) were initially cleaned with piranha solution, a mixture of 30% H_2O_2 and 98% concentration sulfuric acid (both purchased from Fisher scientific) in the ratio 3:7 for 45 min. (***Caution***: *Piranha solution is a strong oxidizing agent, which has*

(17) Montague, M. T.; Ducker, R. E.; Chong, K. S. L.; Manning, R. J.; Rutten, F. J. M.; Davies, M. C.; Leggett, G. J. *Langmuir* **2007**, *23*, 7328.
(18) Sun, S.; Leggett, G. J. *Nano Lett.* **2007**, *7*, 3753.
(19) Hanson, J. R. *Protecting Groups in Organic Synthesis*; Sheffield Academic Press, Black Science, 1999.
(20) Givens, R. S.; Conrad, P. G., II; Yousef, A. L.; Lee, J. I. *Handbook of Organic Photochemistry and Photobiology*, 2nd ed.; CRC Press LLC, 2004.
(21) Beier, M.; Stephan, A.; Hoheisel, J. D. *Helv. Chim. Acta* **2001**, *84*, 2089.
(22) Beier, M.; Hoheisel, J. D. *Nucleic Acids Res.* **2000**, *28*, e11.
(23) Dendane, N.; Hoang, A.; Guillard, L.; Defrancq, E.; Vinet, F.; Dumy, P. *Bioconjugate Chem.* **2007**, *18*, 671.
(24) Pelliccioli, A. P; Wirz, J. *Photochem. Photobiol. Sci.* **2002**, *1*, 441.
(25) Kobayashi, Y.; Sakai, M.; Ueda, A.; Maruyama, K.; Saiki, T.; Suzuki, K. *Anal. Sci.* **2008**, *24*, 571.
(26) Millaruelo, M.; Eng, L. M.; Mertig, M.; Pilch, B.; Oertel, U.; Opitz, J.; Sieczkowska, B.; Simon, F.; Voit, B. *Langmuir* **2006**, *22*, 9446.
(27) Bardecker, J. A.; Afzali, A.; Tulevski, G. S.; Graham, T.; Hannon, J. B.; Jen, A. K.-Y. *J. Am. Chem. Soc.* **2008**, *130*, 7226.
(28) Patchornik, A.; Amit, B.; Woodward, R. B. *J. Am. Chem. Soc.* **1970**, *92*, 6333.
(29) Holmes, C. P.; Solas, D. W.; Kiangsoontra, B. International Pat. Appl. WO9410128, 1994.
(30) Hasan, A.; Stengle, K.; Giegrich, H.; Cornwell, P.; Isham, K. R.; Sachleben, R. A.; Pfleiderer, W.; Foote, R. S. *Tetrahedron* **1997**, *53*, 4247.
(31) Bhusan, K. R.; DeLisi, C.; Laursen, R. A. *Tetrahedron Lett.* **2003**, *44*, 8585.

Scheme 2. Schematic Diagram Showing the Formation of Photolabile Monolayers, Their Photopatterning, and Subsequent Derivatization with (a) Trifluoroacetic Anhydride (TFAA) and (b) Aldehyde-Functionalized Nanoparticles

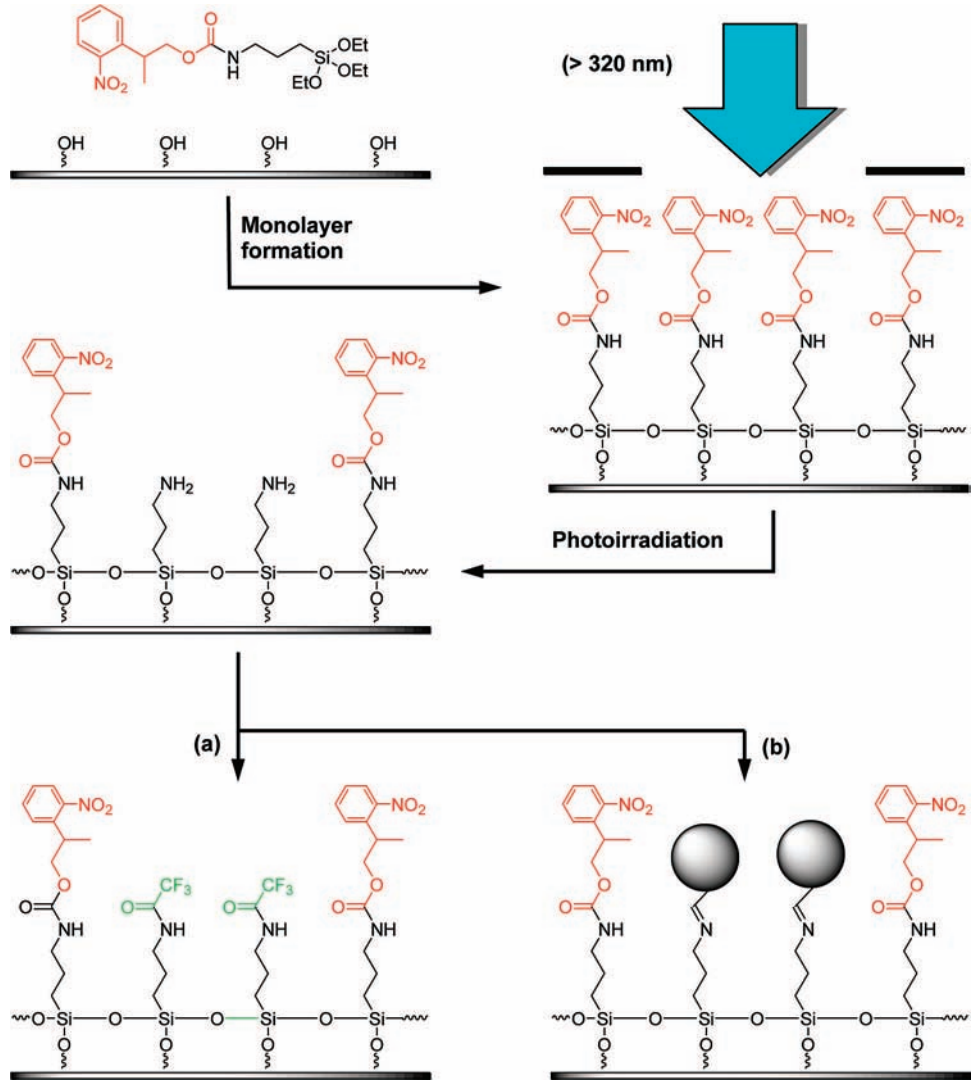

Scheme 3. Synthesis of *N*-NPPOC 3-Aminopropyltriethoxysilane[a]

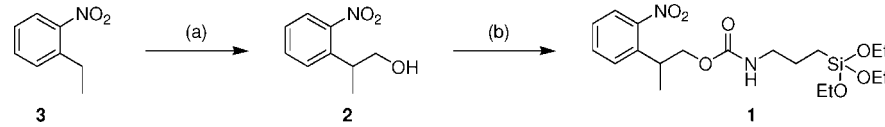

[a] Reagents and conditions: (a) paraformaldehyde, benzyltrimethylammonium hydroxide (Triton B), MeOH, 80 °C, 24 h, 48%; (b) 3-isocyanatopropyltriethoxysilane, Et_3N (9% mol equiv), DCM, 60 °C, 24 h, 75%.

been known to detonate spontaneously upon contact with organic material, and should be handled with extreme care.) Subsequently, they were immersed in an RCA (Radio Cooperative America) cleaning solution (a mixture consisting of ammonium hydroxide (Analar), hydrogen peroxide, and deionized water (Elga Pure Nanopore, 18.2 MΩ) in the ratio of 1:1:5 at 80 °C) for 40 min. The substrates were finally rinsed with ultrapure water and dried in an oven. Aldehyde-coated 100 nm diameter nanoparticles (Duke Scientific, Palo Alto, CA; polystyrene microspheres, 4% solids) were supplied in an ethanolic suspension.

Synthesis. 2-(2-Nitrophenyl)propan-1-ol, 2. This was first synthesized according to previously reported procedures,[31] although the reported yields could not be reproduced. To a 40% benzyltrimethylammonium hydroxide (Triton B) solution in MeOH (17 g of solution, 40.6 mmol) was added 2-ethylnitrobenzene **3** (5400 μL, 40.0 mmol) followed by paraformaldehyde (1267 mg, 40.5 mmol). The mixture was refluxed at 80 °C for 20 h, evaporated under reduced pressure to a small volume, and adjusted to pH 7 with 1 M aq HCl (~40 mL). The mixture was extracted thrice with EtOAc (50 mL each), and the organic layers were combined, dried with $MgSO_4$, and evaporated under reduced pressure to give a brown oil. This was purified by flash column chromatography (hexanes/EtOAc, 4:1 2:1) to yield the desired product as a deep orange oil[31] (3518 mg, 19.42 mmol, 48%) (Scheme 3); R_f 0.11 (hexanes/EtOAc, 4:1); ν_{max}(neat)/cm^{-1} 3373 (OH), 2971 (alkyl), 2874 (alkyl), 1523 ($ArNO_2$), 1349 ($ArNO_2$), 1034 (Ar), 668 (Ar); NMR data conformed to literature;[31] *m*/*z* (CI) 199 (100%, $[M + NH_4]^+$).

{*N*-[2-(2-Nitrophenyl)propan-1-oxycarbonyl]-3-aminopropyl}-triethoxysilane, 1. 2-(2-Nitrophenyl)propan-1-ol **2** (3518 mg, 19.42 mmol) was dissolved in DCM (15 mL), 3-isocyanatopropyltri-

ethoxysilane (5 mL, 20.2 mmol) was added, followed by Et_3N (235 μL, 1.7 mmol), and the mixture refluxed at 60 °C for 24 h. Et_2O (20 mL) was added, and the mixture extracted with 0.1 M potassium phosphate buffer pH 7 (50 mL thrice). The organic layer was dried with $MgSO_4$ and evaporated under reduced pressure, and the residual yellow oil was purified by flash column chromatography (hexanes/EtOAc, 3:1 2:1) to yield the desired product as a yellow oil (6020 mg, 14.05 mmol, 72%); R_f 0.50 (hexanes/EtOAc, 1:1); ν_{max}(neat)/cm^{-1} 3337 (OCONH), 2971 (alkyl), 2928 (alkyl), 2881 (alkyl), 1718 (OCONH), 1526 (NO_2), 1356 (NO_2), 1074 (SiOEt), 954 (SiOEt); δ_H (300 MHz, $CDCl_3$) 0.59 (2H, t, *J* 8, C*H*$_2$Si), 1.21 (9H, t, *J* 7, OCH$_2$C*H*$_3$), 1.34 (3H, d, *J* 7, C*H*$_3$CH), 1.58 (2H, tt, *J* 7 and 8, CH$_2$C*H*$_2$CH$_2$), 3.12 (2H, td, *J* 7 and 6, NHC*H*$_2$), 3.70 (1H, m, CH$_3$C*H*), 3.81 (6H, q, *J* 7, SiOC*H*$_2$), 4.10 (1H, m, CHC*H*$_2$O), 4.23 (1H, m, CHC*H*$_2$O), 4.85 (1H, s(br), CON*H*CH$_2$), 7.36 (1H, dd, *J* 8 and 8, 5-Ph), 7.47 (1H, d, *J* 8, 3-Ph), 7.56 (1H, dd, *J* 8 and 8, 4-Ph), 7.73 (1H, d, *J* 8, 6-Ph); δ_C (100 MHz, $CDCl_3$) 7.9 (*C*H$_2$Si), 17.8 (*C*H$_3$CH), 18.7 (OCH$_2$*C*H$_3$), 23.6 (CH$_2$*C*H$_2$CH$_2$), 33.6 (CH$_3$*C*H), 43.7 (NH*C*H$_2$), 58.8 (O*C*H$_2$CH$_3$), 68.9 (CH*C*H$_2$O), 124.4 (6-Ph), 127.6 (5-Ph), 128.3 (3-Ph), 132.9 (4-Ph), 137.9 (2-Ph), 151.1 (1-Ph), 156.5 (O*C*ONH); *m*/*z* (ES+) 451 (100%, [M + Na]$^+$); HRMS found 451.1875 [M + Na]$^+$, requires 451.1871, δ 0.9 ppm.

Sample Preparation. A 1 cm^2 piece of the silicon oxide substrate was placed in a Schlenck tube, fitted with a septum, evacuated to 10 mbar, and filled with a dry nitrogen atmosphere. A 1 mM solution of NPPOC−silane was prepared in toluene and left for varying time periods to enable monitoring of the change in surface coverage. After completion of the reaction, the samples were rinsed with toluene, then ethanol, and dried under a stream of nitrogen to avoid cross-contamination prior to placing in a vacuum oven for 45 min.

Surface Photochemistry and Patterning. Photodeprotection of NPPOC was conducted using light from He−Cd (325 nm, Kimmon IK3202R-D) or Ar-ion (364 nm, Coherent Innova I328, Coherent, Santa Clara, CA) lasers. For micropatterning, 1500 and 1000 mesh (i.e., lines per inch) electron microscope grids (Agar, Cambridge, U.K.) were used as masks and the laser power was 11 mW. To investigate the kinetics of photodeprotection, the laser beam was defocused to irradiate an area of 0.5 cm^2. For nanoscale patterning, the lasers were coupled to a Witec AlphaSNOM (WiTec, Ulm, Germany). Microstructured cantilever sensors, consisting of a rectangular cantilever, with a hollow pyramidal tip at one end, were used. An optical deflection feedback system was employed. The tips had 100 nm apertures at their apexes, into which UV light was focused using a 0.2 numerical aperture lens.

Sample Derivatization. Derivatization reactions were carried out after the samples were exposed to UV light, rinsed with ethanol, dried in a stream of N_2, and placed in Schlenck tubes under a dry N_2 atmosphere. For TFAA derivatization, the samples were immersed in 20 mM solution of the reagent in anhydrous THF, with twice the molar quantity of triethylamine. The immersion time was varied from 5 min to 3 h. Derivatization with aldehyde-functionalized nanoparticles was carried out by coating the surface in 30 μL of nanoparticle suspension for 30 min. All the derivatized samples were then analyzed by atomic force microscopy (AFM).

Surface Analysis. Advancing sessile drop contact angle measurements were made using a Rame-Hart model 100-00 goniometer (Netcong, NJ). Contact and tapping mode AFM images were acquired using a Multimode atomic microscope with a Nanoscope IIIA controller (Veeco, Santa Barbara, CA). Silicon nitride probes with average spring constants of 0.06 and 0.12 Nm^{-1}, and nominal tip radii of between 20 and 60 nm, were used for contact mode measurements, and silicon probes (Veeco TESP probes) were used for tapping mode measurements. Ellipsometry was carried out using a Jobin-Yvon UVISEL spectroscopic ellipsometer (Longjumeau, France), at an incident angle of 70°, in the range of 200−850 nm. The data were collected and averaged over at least three different areas for each of the samples. To calculate the film thickness, a refractive index of 1.5 was assumed for all polymer layers and a Cauchy absorbent algorithm was utilized.

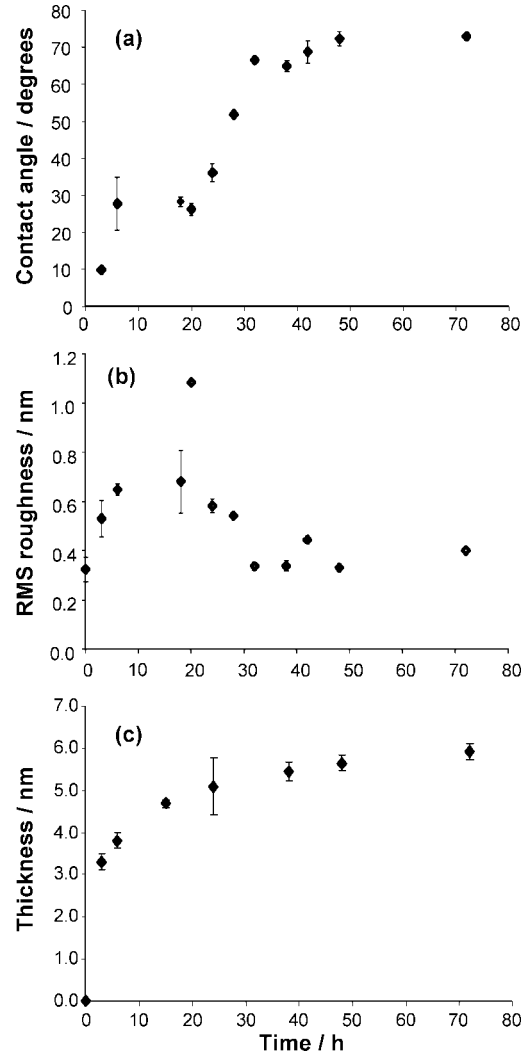

Figure 1. Variation in the advancing water contact angle (a), roughness (b), and thickness (c) as a function of time of immersion of glass substrates in a solution of the NPPOC-protected silane.

X-ray photoelectron spectroscopy (XPS) analyses were performed using a Kratos Axis Ultra X-ray photoelectron spectrometer (Kratos, Manchester, U.K.), equipped with a monochromatic Al Kα X-ray source operating with a base pressure in the range of 10^{-8} to 10^{-10} mbar. An electron energy analyzer pass energy of 80 eV was used for high-resolution scans, and data were processed using CasaXPS software (http://www.casaxps.com/). All binding energies were referenced to the main hydrocarbon peak, set at a binding energy of 285 eV. Peaks were fitted with a linear background, using symmetrical Voigt-type functions, with contributions from both Gaussian and Lorentzian profiles (typically in the proportion 90% Gaussian to 10% Lorentzian).

Results and Discussion

Film Preparation. Siloxane films are typically complex, and the quality of the resulting materials depends upon a variety of parameters.[32−34] Under controlled conditions of humidity, as employed here, the time of exposure of the substrate to the silane solution is important. To establish the time required to achieve uniform coverage of the surface by the NPPOC-protected silane, measurements were made of the root mean squared (rms) surface roughness, contact angle, and thickness as a function of exposure time (Figure 1).

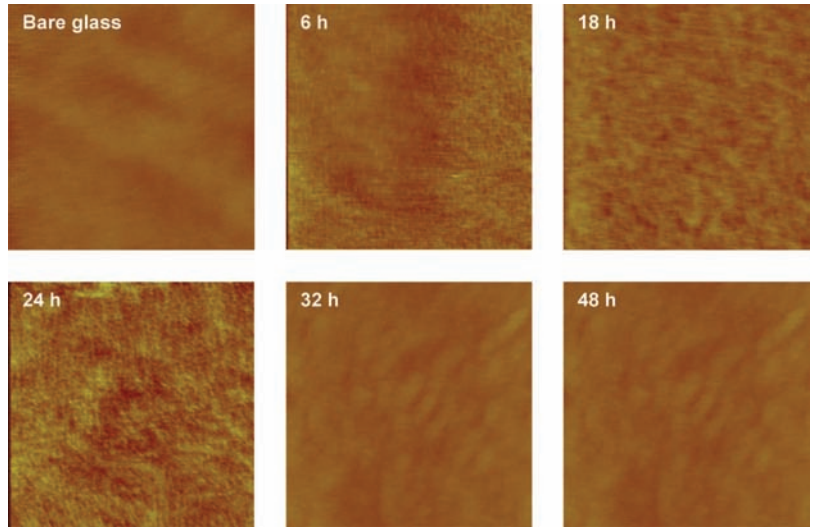

Figure 2. Height images of NPPOC−aminosiloxane films deposited for varying times. Image size: 1 μm × 1 μm. The z-range is 25 nm in each case.

The water contact angle of the unmodified substrate was found to be less than 10°. After immersion in the NPPOC-protected silane solution, the contact angle data showed a gradual rise, with the rate of change decreasing after 30 h and reaching a maximum constant value of 75° after 48 h. The change in contact angle was attributed to a gradual increase in the surface coverage, and the attainment of a limiting value for the contact angle was attributed to the formation of a full-coverage film. In comparison to the highly reactive trichlorosilanes that tend to achieve complete coverage more rapidly, the prolonged deposition time required here is attributed to the less reactive nature of the triethoxysilane used here, which is hydrolyzed in solution, in agreement with the observations of Dendane et al.[23]

Figure 1b shows the relationship between the roughness of the samples and immersion time. The roughness increased to ca. 0.7 nm over 12 h, then decreased again, before reaching a limiting value of ca. 0.4 nm at immersion times in excess of 40 h. The most likely explanation for these observations is that initial growth of the monolayer occurs through island formation. As islands grow, the roughness increases, but eventually the islands begin to coalesce and form larger structures, at which point the roughness begins to decrease until complete coverage is formed. Visual inspection of height images acquired by AFM (Figure 2) supports this hypothesis. Here, the featureless glass substrate is replaced by a textured morphology after 6 h of immersion, but after 32 h, large features are observed that exhibit a relatively smooth morphology. On the basis of both the contact angle and the AFM data, it is clear that after 48 h the surface has reached a limiting composition and morphology. For subsequent experiments, the substrates were thus prepared by immersion in the NPPOC-protected silane solution for 48 h.

Measurements by ellipsometry (Figure 1c) showed that the thickness of the NPPOC-protected films increased with the time of immersion in the siloxane solution, rising rapidly to reach a thickness of 3.2 nm after 3 h and rising more slowly to reach a limiting value after ca. 48 h. The limiting thickness was found to be 5.5 nm, consistent with the formation of a film ca. two layers thick.

The full-coverage NPPOC-protected films were then characterized by XPS. The survey spectrum (not shown) exhibited peaks at 285, 99, 400, and 532 eV corresponding to C1s, Si2p, N1s, and O1s. Although silicon and oxygen were present in the NPPOC-protected silane adsorbate, the Si2p and O1s peaks also contained substantial contributions from the underlying silicon wafer substrates, and these atomic concentrations were not useful for characterizing films. Instead, high-resolution spectra were acquired for the C1s and N1s regions and are shown in Figure 3. The predominant peak in the C1s spectrum was located at 285.2 eV, with carbons attached to nitrogen and oxygen components observed at 286.5 eV and a slight hint of the carbamate carbon signal at 289.3 eV. In Figure 3b, two bands are observed in the N1s region. The peaks at 400.0 and 406.2 eV are assigned to the nitrogen atoms in the amine and nitro groups, respectively, consistent with experimental and theoretical studies.[35]Deconvolution of the band confirmed that the two components were present in approximately equal intensity, as expected.

The stability of the films was tested using XPS (see the Supporting Information). Samples stored in the dark yielded unchanged N1s spectra even after 45 days of exposure to the atmosphere. When no effort was made to protect samples from light, a reduction was observed in the area of the nitro-group component in the N1s spectrum after storage for 24 h. For samples stored in neutral and acidic (pH 2) solutions, to test their utility for subsequent functionalization, the N1s spectrum was found to be unchanged after 24 h. In strongly basic conditions (pH 12), a reduction was observed in the area of the nitro component in the XPS spectrum after 2 h. Broadly, these data indicate that the NPPOC-protected films offer exceptional stability.

Photodeprotection. The removal of the NPPOC protecting group requires irradiation with light which has a wavelength longer than 320 nm.[27] In the present work, two wavelengths were used, 325 and 364 nm, produced by He−Cd and Ar-ion

(32) Rozlosnik, N.; Gerstenberg, M. C.; Larsen, N. B. *Langmuir* **2003**, *19*, 1182.
(33) Cras, J. J.; Rowe-Taitt, C. A.; Nivens, D. A.; Ligler, F. S. *Biosens. Bioelectron.* **1999**, *14*, 683.
(34) McGovern, M. E.; Kallury, K. M. R.; Thompson, M. *Langmuir* **1994**, *10*, 3607.
(35) La, Y.-H.; Kim, H. J.; Maeng, S.; Jung, Y. J.; Park, J. W. *Langmuir* **2002**, *18*, 2430.

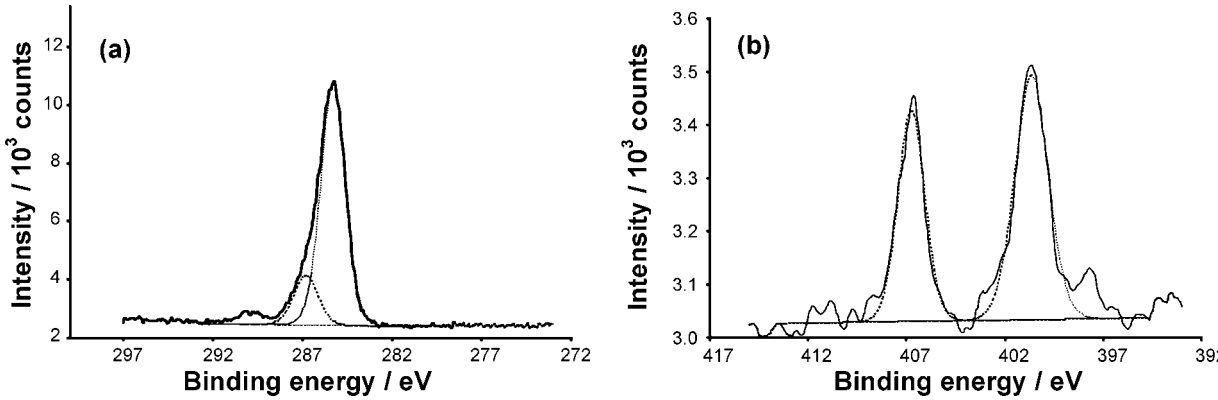

Figure 3. XPS spectra of the NPPOC−aminosilane monolayer: (a) high-resolution C1s spectrum; (b) high-resolution of N1s spectrum.

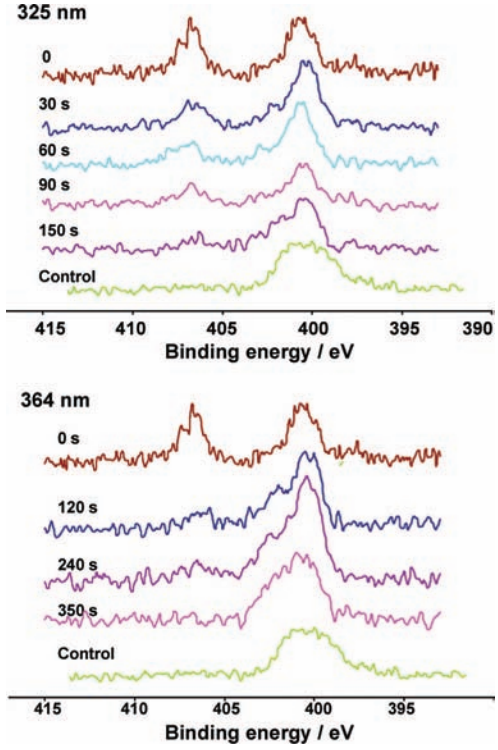

Figure 4. Variation in the N1s region of the XPS spectrum as a function of UV exposure at 325 and 364 nm. The control spectrum is for a film of aminopropyltriethoxysilane.

lasers (respectively). It was expected that irradiation of NPPOC-protected surfaces with UV light should result in the formation of free amine groups on the surfaces and with concomitant release of the nitrophenylalkene byproduct and carbon dioxide (Scheme 1). Thus, XPS analysis was used to monitor the changes in the N1s spectra. Figure 4 shows the variation in the N1s region of the XPS spectrum as a function of UV exposure at both 325 and 364 nm. It was found that the nitro component of the spectrum decreased rapidly in intensity following exposure to UV light, consistent with the removal of the protecting group.

Figure 5a shows the variation in the ratio of the NO_2 to NH_2 components in the N1s spectrum with exposure at 325 and 364 nm. For both wavelengths, a rapid fall was observed, with a greater rate of change being observed for exposure at 325 nm than was observed following exposure at 364 nm. At neither wavelength did the intensity of this ratio decrease to zero, however. The most likely explanation for this is that the siloxane film was thicker than a monolayer, in agreement with the data in Figure 1. Ellipsometry measurements suggested that, after photodeprotection, the film thickness reduced by ca. 2 nm, consistent with the deprotection of the topmost layer of siloxanes (see the Supporting Information). Mechanisms of siloxane film formation are known to be complex, and multilayer formation has been widely reported. Although the XPS data indicate extensive elimination of the nitro byproduct, it is possible that if the first layer of adsorbates is covered with a silane overlayer, deprotection is not followed by removal of the nitro-functionalized product yielding a residual component in the N1s spectrum.

Figure 5b also shows the variation in the water contact angle of the NPPOC-protected silane films following irradiation. At both wavelengths, the contact angle fell rapidly, from an initial value of 75°. For irradiation at 325 nm, a limiting value of just less than 60° was reached after an exposure of 1.2 J cm^{-2}, consistent with the conversion of the NPPOC groups to the more polar amines. The contact angles for samples irradiated at 364 nm decreased slightly more slowly, but the data indicated that a significant degree of deprotection had nevertheless already occurred after an exposure of 1.2 J cm^{-2}.

Micropatterning of Siloxane Monolayers. Samples of the NPPOC-protected siloxane films were exposed to UV light through masks in order to create micrometer-scale patterns. Friction force microscopy (FFM) was used to characterize the effect of irradiation on surface composition (Figure 6). It can be seen from Figure 6 that the exposed areas (squares) yielded brighter contrast than the masked areas (bars). The increase in contrast observed in the exposed areas, reflecting an increase in the friction force due to an increasing strength of interaction between the AFM probe and the amine groups produced by photodeprotection, is in agreement with an extensive body of literature correlating frictional behavior with surface free energy for organic materials.[36,37] The clarity of contrast was notable, given the rather modest change in contact angle associated with the deprotection step

Surface Reactivity Following Photodeprotection. Sample surfaces were treated with a 20 mM solution of trifluoroacetic anhydride (TFAA) in THF, following photodeprotection, to give trifluoroacetamide-functionalized patterns and characterized by contact angle measurement and XPS. Reaction between the

(36) Beake, B. D.; Leggett, G. J. *Langmuir* **2000**, *16*, 735.
(37) Leggett, G. J.; Brewer, N. J.; Chong, K. S. L. *Phys. Chem. Chem. Phys.* **2005**, *7*, 1107.

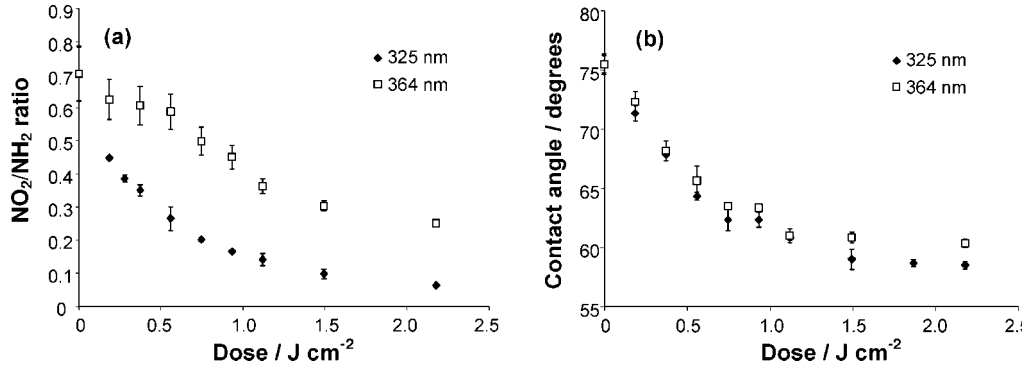

Figure 5. Variation in the ratio of the amine- and nitro-group components in the N1s spectrum (a) and water contact angle (b) following continuous irradiation of NPPOC-protected silane films at wavelengths of 325 and 364 nm.

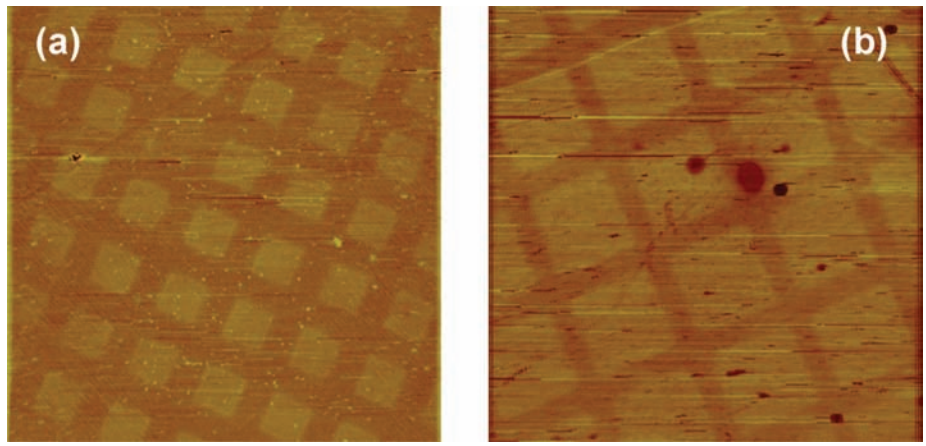

Figure 6. 100 μm $\times$ 100 μm FFM images of photopatterned NPPOC monolayers exposed to light with wavelengths of (a) 325 and (b) 364 nm.

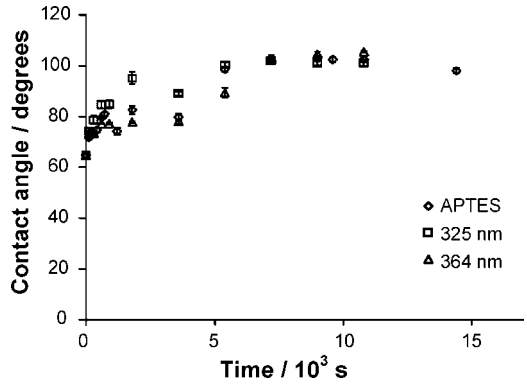

Figure 7. Variation in the advancing water contact angle with immersion time in a solution of TFAA for a control sample, APTES, and for NPPOC monolayers deprotected by illumination at 325 and 364 nm.

anhydride and the deprotected amine was expected to yield an amide bond. To test whether the behavior was commensurate with complete deprotection of the surface, control samples were prepared by the adsorption of aminopropyltriethoxysilane (APTES) onto glass surfaces and these control samples were reacted with TFAA following the same procedure used for the photodeprotected silane samples.

Figure 7 shows the variation in the advancing water contact angles as a function of the time of immersion in a TFAA solution of NPPOC-protected samples following deprotection, by exposure to a dose of 1.2 J cm^{-2} at both 325 and 364 nm, and for APTES films. The observed data for all three data sets are essentially indistinguishable. The contact angles of all samples rose rapidly, initially, and then the rate of change slowed until they eventually reached an equal limiting value of 102° after a time of 5400 s. There was no further change in the contact angle after 3 h. The value obtained here for complete derivatization agrees closely with measurements made for hydroxyl-terminated SAMs of alkanethiols on gold.[38,39]

The C1s XPS spectra obtained for derivatized films of the NPPOC-protected silane following photodeprotection at both 325 and 364 nm are shown in Figure 8. Table 1 shows the peak assignments. The peaks at 289.3 and 293.2 eV, present in the ratio of 1:1, can be unambiguously attributed to the amide (N$-$C$=$O) and CF_3 and confirm that reaction has taken place between the amine group and the anhydride. The peak at the binding energy of 285.0 eV is attributed to alkyl chain carbons. The survey scan (not shown) yielded elemental intensity ratios C/N/F of 5:1:3, which are close to the expected values for a fully derivatized monolayer. The ratio of the areas of the C$-$N and CF_3 components was not exactly one to one, suggesting 0.68 $\pm$ 0.01 of CF_3 derivatized on surfaces through 2 h of reaction. To examine whether the surface has a complete reaction, irradiated SAMs were exposed to a 5-fold concentration excess of TFAA solution. However, there was no further change in the contact angle even after a reaction time of 3 h. The incomplete derivatization of the molecules is probably due to steric hindrance due to the size of the CF_3 groups.[38] However, perfluorinated organic molecules are also highly susceptible to

(38) Pan, S.; Castner, D. G.; Ratner, B. D. *Langmuir* **1998**, *14*, 3545–3550.
(39) Hutt, D. A.; Leggett, G. J. *Langmuir* **1997**, *13*, 2740.

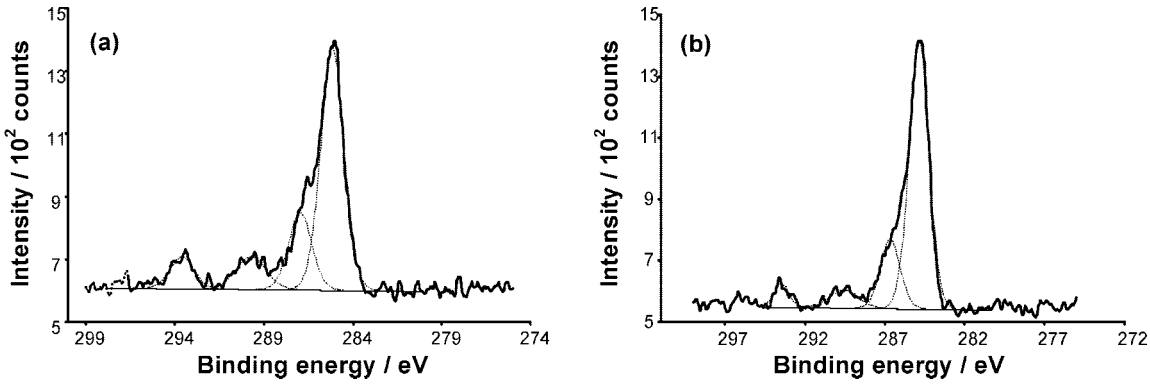

Figure 8. High-resolution C1s XPS spectra of deprotected NPPOC silane monolayers at (a) 325 and (b) 364 nm following exposure to TFAA solution for 2 h.

Table 1. Peaks Representing Various Functional Groups during Deconvolution of the C1s High-Resolution XPS Spectra

functional groups	binding energy (eV)
Si−C	284.5
C−C	285.0
C−F	293.2
C−N	286.5
C═O	289.3

X-ray-induced damage,[40] and this may also contribute to a reduction in the area of the peak due to the CF_3 group. It is certainly clear from these data that derivatization of the photodeprotected films is as extensive as derivatization of the control surface.

Micrometer-scale patterned SAMs were prepared by photodeprotection by exposure to wavelengths of 325 and 364 nm for 180 s and subsequently functionalized with TFAA as described above. The samples were characterized using FFM. Parts a and b of Figure 9 show the resulting images. In the exposed areas (the squares), the contrast is now inverted by comparison with the images in Figure 6, reflecting the fact that the friction force is smaller for the fluorinated regions than for the NPPOC-protected masked areas (the bars). As in Figure 6, it is significant to note that the contrast difference is clear, despite the modest difference in contact angle for the macroscopic samples treated in the same way (25°), emphasizing the utility of FFM as a tool for characterizing changes in surface chemistry with high spatial resolution.

Patterned, photodeprotected monolayers were also derivatized using aldehyde-functionalized polymer nanoparticles. The aldehydes were expected to react with the amine groups produced by photodeprotection to yield imine linkages to the surface. Following photodeprotection as described previously, the samples were immersed in a nanoparticle solution for 30 min and then rinsed with ethanol to remove any nonspecifically bound particles. The samples were then rinsed and imaged with AFM. Height images are shown in Figure 9, parts c and d, together with representative line sections (Figure 9, parts e and f, respectively). There is a clear height contrast between exposed and masked areas. Analysis of the line sections confirmed that the height of the features observed on the exposed areas was 100 nm, corresponding to the diameter of the nanoparticles that had been attached. There was no evidence of reaction with the masked area. This provides further evidence for the existence of amine groups at the surface after deprotection. However, the nanoparticles are not close-packed at the surface in Figure 9, parts c and d. This is attributed to geometric factors: in the absence of a flexible linker, the area on the surface of the nanoparticles that is able to approach the surface and bond with it is extremely small, leading to incomplete coverage. Similar results have been observed in other experiments involving nanoparticles attachment to patterned surfaces.[15,41]

Nanometer-Scale Photopatterning. Nanostructures were fabricated using scanning near-field photolithography (SNP). The UV lasers were coupled to a scanning near-field microscope (SNOM), and the samples were exposed to the optical near field associated with the aperture of the microscope. The microscope used in the present study utilized cantilever-type probes. These probes were similar to conventional AFM probes, but the pyramidal tips were hollow with apertures formed at their apexes. Light from the laser passed along an optical fiber and was focused into the hollow probe using a high numerical aperture lens. Figure 10 shows the results of the nanofabrication experiments.

Initially, photodeprotection of NPPOC-protected surfaces was carried out at wavelengths of 325 and 364 nm and a laser power of 11 mW. The power quoted here is that of the beam prior to coupling to the optical fiber leading to the SNOM; measurement of the intensity of illumination in the near field was not possible. At a scan rate of 0.5 μm s^{-1}, a line width of 150 nm was achieved. Parts a, c, and e of Figure 10 show illustrative FFM data at different magnifications. As was observed in the micrometer-scale patterning experiments, there is clear contrast between the deprotected regions (the lines) and the surrounding surface, and the lines exhibit brighter contrast than the protected areas because the amine groups that result from deprotection of the adsorbate are more polar and hence adhere more strongly to the AFM probe as it scans the sample.

Following immersion of the samples in a solution of TFAA, a contrast inversion was observed, in agreement with the data for micropatterned samples, and the contrast on the lines became dark relative to the surrounding, protected regions (Figure 10, parts b, d, and f) as a result of the amine groups becoming derivatized with the nonpolar fluorinated functional groups. The clarity of the contrast inversion, given the small size of the features and the modest change in contact angle, is striking.

Nanoparticle attachment was also attempted. However, dense structures were not observed. The line widths of the patterns

(40) Graham, R. L.; Bain, C. D.; Biebyuck, H. A.; Laibinis, P. E.; Whitesides, G. M. *J. Phys. Chem.* **1993**, *97*, 9456.

(41) Sun, S.; Chong, K. S. L.; Leggett, G. J. *Nanotechnology* **2005**, *16*, 1798.

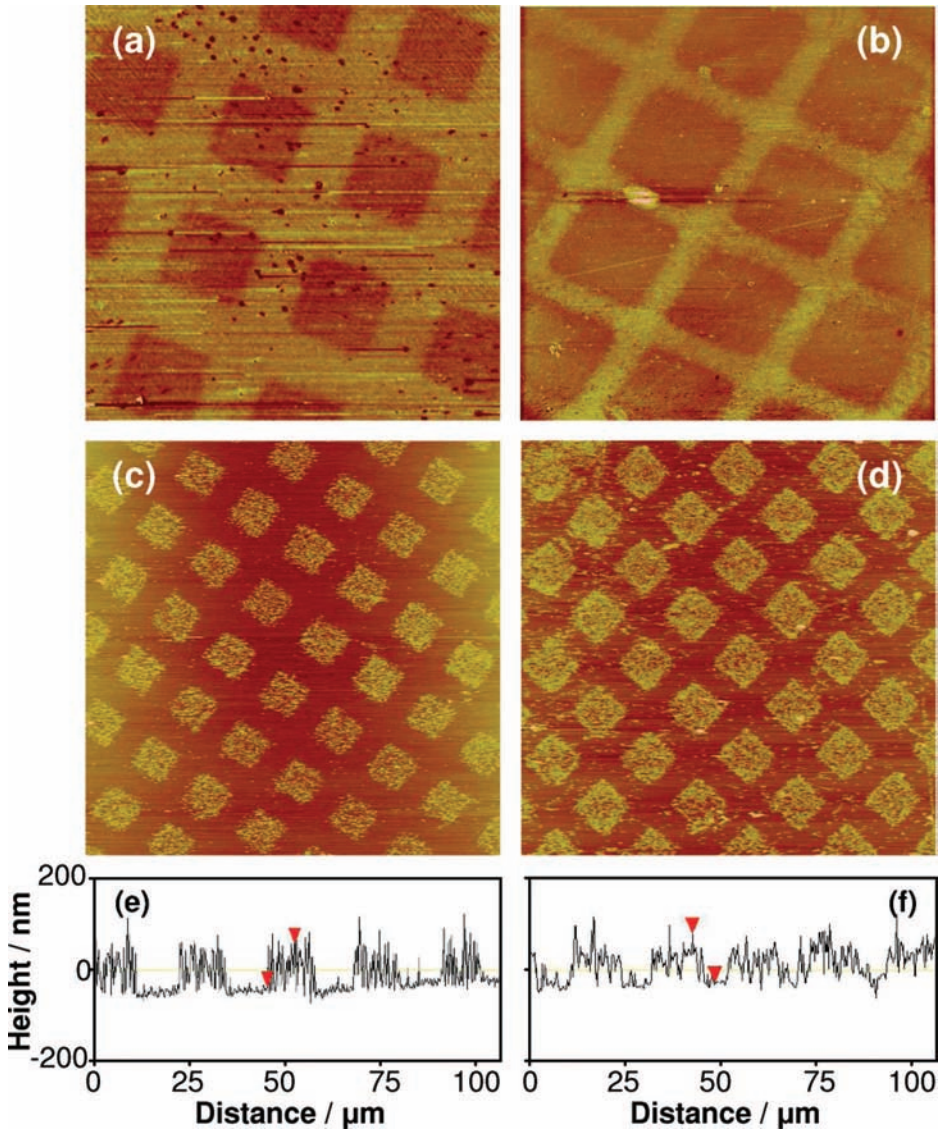

Figure 9. AFM images of derivatized NPPOC-terminated films following patterned photodeprotection at 325 nm (a and c) and 364 (b and d) nm. Panels a and b are 50 μm × 50 μm FFM images of samples that have been derivatized by reaction with TFAA. Panels c and d are 100 μm × 100 μm height images of samples that have been derivatized by attachment of aldehyde-functionalized polymer nanoparticles, and panels e and f show lines sections through panels c and d, respectively.

formed by SNP were smaller than the diameters of the particles employed, and given the tendency of the nanoparticles not to form close-packed structures following attachment to the surface, the reduced packing density following incubation with nanopatterned samples was expected.

The resolution achieved here is not as good as has previously been reported in studies of monolayers of alkanethiols on gold or chloromethylphenylsilane monolayers on silicon. However, the aperture diameter in the commercial probes used here (ca. 100 nm) was significantly greater than that of the probes used in those studies (ca. 50 nm). It is therefore expected that significant improvements in resolution would be feasible for the NPPOC system for probes with smaller apertures.

It is plain from Figures 5 and 6 that the photodeprotection of the NPPOC-protected films was rapid. It proved possible to write nanostructures at elevated speeds using SNP. Photodeprotection was efficient at speeds as high as 20 μm s^{-1}, an order of magnitude faster than previously achieved for thiol monolayer systems.

The above data clearly demonstrate that NPPOC-protected monolayers provide a very straightforward means to produce patterned molecular structures when combined with a suitable photopatterning method. Given the wide range of methods available for the derivatization of amine groups, the method promises to be one that has widespread utility in the fabrication of functional molecular architectures, with resolutions ranging from the macroscopic to the nanometer scales. In earlier work on SNP, we have relied upon deep-UV excitation, with the consequence that expensive laser systems and optics are required. However, the availability of a versatile system that undergoes photochemical modification on exposure to near-UV light promises to extend the methodology substantially and give it much wider utility.

Conclusions

Films of *N*-NPPOC 3-aminopropyltriethoxysilane may readily be formed. Contact angle and AFM measurements indicate that the adsorbates initially nucleate to form islands, which grow in

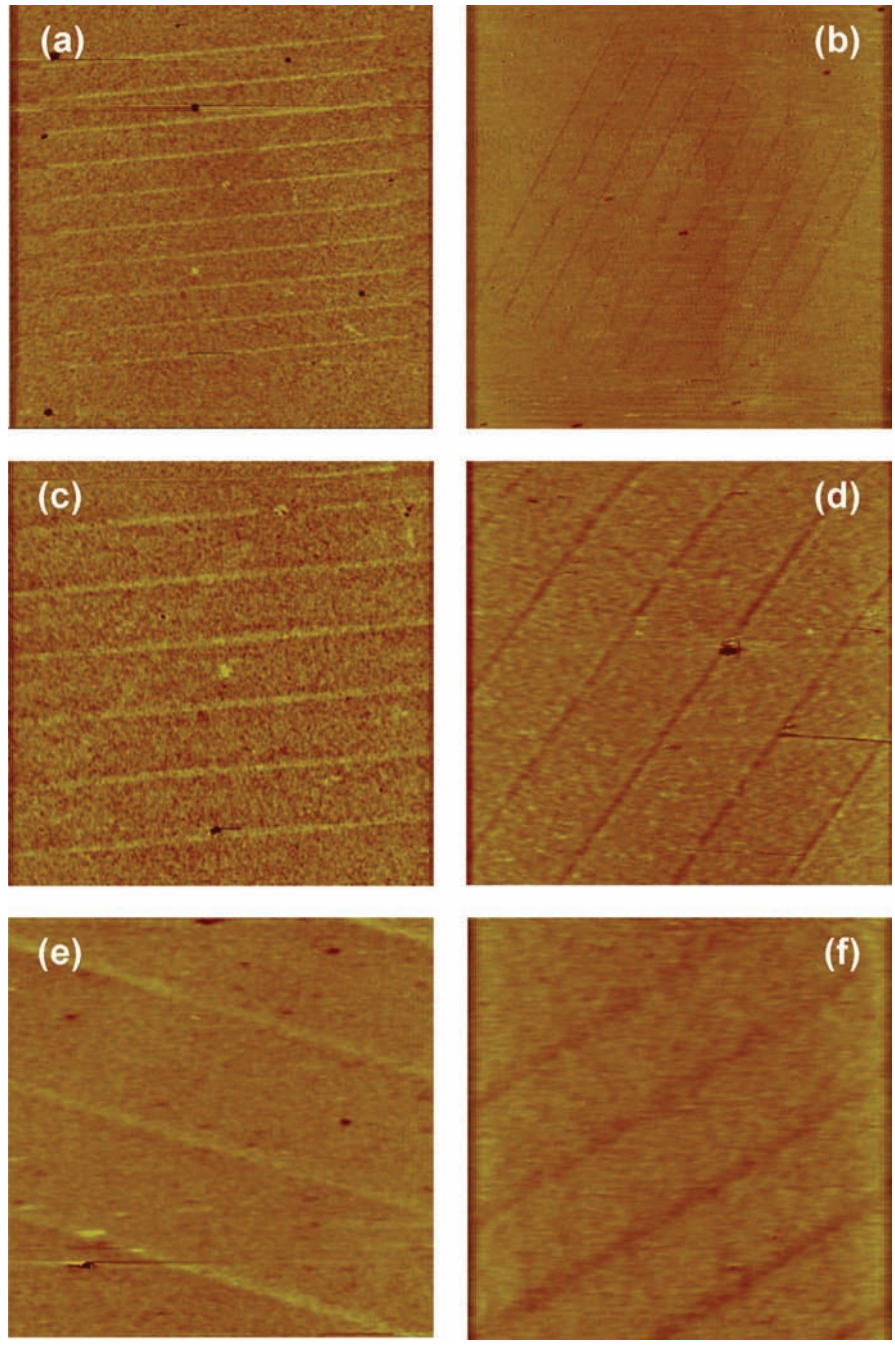

Figure 10. Friction force microscopy images of nanopatterned irradiated at wavelengths of 325 nm (a−d) 325 nm and 364 nm (e and f). Images a, c, and e were acquired directly following exposure of the sample to the near-field probe, and images b, d, and f were acquired following derivatization using TFAA. Image sizes: (a) 60 × 60 μm^2; (b) 33 × 33 μm^2; (c) 20.0 × 20.0 μm^2; (d) 11 × 11 μm^2; (e) 12 × 12 μm^2; (f) 11 × 11 μm^2.

size with time, eventually coalescing to form a continuous film with low roughness after 48 h. Photodeprotection may be carried out at either 325 or 364 nm, to yield an amine-functionalized surface. Photodeprotection is extremely rapid. The deprotected surfaces react with trifluoroacetic anhydride to yield extensively derivatized surfaces that are indistinguishable from those formed by derivatization of aminopropyltriethoxysilane control surfaces. Exposure of the sample through a mask yields a pattern, which may be imaged by friction force microscopy. TFAA derivatization causes an inversion of the FFM contrast. The surface may also be efficiently derivatized using aldehyde-functionalized polymer nanoparticles. Nanometer-scale patterns may be formed by coupling the laser light source to a scanning near-field optical microscope. A resolution of 150 nm has been achieved, with a maximum writing rate of 20 $\mu m\ s^{-1}$.

Acknowledgment. S.A.A.A. thanks the Malaysian Government for a research scholarship. The authors thank Research Councils U.K. (Grant No. EP/C523857/1) for financial support.

Supporting Information Available: XPS data on the stability of NPPOC-protected siloxane films under ambient and aqueous conditions and ellipsometric data acquired following UV deprotection of NPPOC-protected films. This material is available free of charge via the Internet at http://pubs.acs.org.

JA807612Y